



CHORUS

This is the accepted manuscript made available via CHORUS. The article has been published as:

Magnetism in Closed-Shell Quantum Dots: Emergence of Magnetic Bipolarons

Rafał Oszwałdowski, Igor Žutić, and A. G. Petukhov

Phys. Rev. Lett. **106**, 177201 — Published 25 April 2011

DOI: [10.1103/PhysRevLett.106.177201](https://doi.org/10.1103/PhysRevLett.106.177201)

Magnetism in Closed-shell Quantum Dots: Emergence of Magnetic Bipolarons

Rafał Oszwałdowski,¹ Igor Žutić,¹ and A. G. Petukhov²

¹*Department of Physics, University at Buffalo, NY 14260-1500, USA and*

³*South Dakota School of Mines and Technology, Rapid City, SD 57701, USA*

Abstract

Similar to atoms and nuclei, semiconductor quantum dots exhibit formation of shells. Predictions of magnetic behavior of the dots are often based on the shell occupancies. Thus, closed-shell quantum dots are assumed to be inherently nonmagnetic. Here, we propose a possibility of magnetism in such dots doped with magnetic impurities. On the example of the system of two interacting fermions, the simplest embodiment of the closed-shell structure, we demonstrate the emergence of a novel broken-symmetry ground state that is neither spin-singlet nor spin-triplet. We propose experimental tests of our predictions and the magnetic-dot structures to perform them.

PACS numbers: 75.50.Pp, 75.75.Lf, 85.75.-d, 73.21.La

Formation of shell structure is a ubiquitous feature in finite fermionic systems, such as atoms, nuclei, and quantum dots (QDs) [1]. An effective potential, in which the fermions are assumed to move independently, can be attributed to the underlying mean field, arising from an interplay of particle-particle interaction and confinement. Open-shell atoms, e.g., Ag and Fe, undergo a spontaneous symmetry breaking of the mean field and are magnetically active due to their spin-polarized ground state (GS). For open-shell QDs doped with transition-metal atoms, typically Mn, strong exchange coupling between a carrier spin and the impurity spin is expected [2–4]. Such QDs exhibit magnetic ordering, which persists even up to room temperature [5–7]. In contrast, closed-shell fermionic systems, e.g., noble gases, are known for their stability and the total spin-zero GS, making them magnetically inert [8].

According to a theorem by Wigner [9], the GS of any non-magnetic two-electron system, including a two-electron QD, is a spin-singlet. Thus, it would seem that closed-shell QDs doped with Mn do not allow magnetic ordering. However, on the example of a two-particle (two electrons or holes) system, we show that the Mn doping does alter the magnetic properties of closed-shell QDs. Surprisingly, we find a GS, which is neither a singlet nor a triplet, and allows ordering of Mn-spin, owing to the spontaneously broken time-reversal symmetry [10]. This mechanism of magnetism is different than in the open-shell systems, such as bulk (Ga,Mn)As or (Cd,Mn)Te [11]. By definition, the open-shell systems have more of either "spin-up" or "spin-down" carriers. This is in contrast to the magnetic closed-shell state considered here, characterized by zero total spin projection.

Carriers confined in a QD interact with magnetic ions via contact exchange interaction, described by

$$H_{ex} = - (J_{ex}/N_0) \sum_{ij,\alpha\beta} \hat{s}_{i\alpha} g_{\alpha\beta} \hat{S}_{j\beta} \delta(\mathbf{r}_i - \mathbf{R}_j), \quad (1)$$

where N_0 is the cation density. The exchange integral, J_{ex} , is typically ~ 0.1 eV for electrons, and ~ -1 eV for holes. Carrier and magnetic ion positions are denoted by \mathbf{r}_i and \mathbf{R}_j respectively; $\hat{\mathbf{S}}$ and $\hat{\mathbf{s}}$ are the Mn and carrier spins. g -tensor describes possible exchange-coupling anisotropy, which is caused by spin-orbit interaction combined with the quasi-two-dimensional shape of QDs. In many semiconductors, this anisotropy is almost negligible for electrons. In contrast, for confined holes, the spin-orbit coupling leads to a strong anisotropy with "easy axis" along the growth direction z [12]. Thus, Eq. (1) reduces to the Ising Hamiltonian for the heavy hole $\pm 3/2$ pseudospin subspace.

We focus on a two-carrier QD, the simplest example of a closed-shell system. The total Hamiltonian, $H = H_f + H_{ex}$, contains the fermionic part H_f , which employs a typical two-dimensional (2D) model for two carriers in a QD [13], $H_f = -\hbar^2/(2m^*) (\nabla_1^2 + \nabla_2^2) + m^*\omega_0^2 (r_1^2 + r_2^2)/2 + e^2/(4\pi\epsilon r_{12})$, where \hbar is the Planck constant, m^* the effective mass, ω_0 determines the 2D confinement, e is the electron charge, ϵ the QD's dielectric constant, and $r_{12} = |\mathbf{r}_1 - \mathbf{r}_2|$. The Coulomb interaction is characterized by the effective Rydberg energy $Ry^* = m^*e^4/[32(\pi\epsilon\hbar)^2]$. We express the two-fermion wavefunction Φ as

$$\Phi = \sum_{\sigma, \sigma'} \varphi_{\sigma\sigma'}(\mathbf{r}_1, \mathbf{r}_2) \chi_{\sigma}(1) \otimes \chi_{\sigma'}(2). \quad (2)$$

Here $\chi_{\sigma}(1)$ and $\chi_{\sigma}(2)$ are spinors of the carriers 1 and 2, and $\sigma = \pm 1/2$ (or \uparrow, \downarrow) correspond to the spin projection along the quantization axis z . The Pauli principle requires $\varphi_{\sigma\sigma'}(\mathbf{r}_1, \mathbf{r}_2) = -\varphi_{\sigma'\sigma}(\mathbf{r}_2, \mathbf{r}_1)$. Thus, $\varphi_{\uparrow\uparrow}$ and $\varphi_{\downarrow\downarrow}$ must be antisymmetric functions of \mathbf{r}_1 and \mathbf{r}_2 , while $\varphi_{\uparrow\downarrow}(\mathbf{r}_1, \mathbf{r}_2)$ and $\varphi_{\downarrow\uparrow}(\mathbf{r}_2, \mathbf{r}_1)$ transform into each other and could be neither symmetric nor antisymmetric. To understand the origin of these states, we first consider the



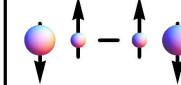
state	orbital	spin	wavefunction
singlet (S)	symmetric	antisymmetric	
triplet (T)	antisymmetric	symmetric	
pseudo-singlet (PS)	not separable		

FIG. 1. (color online) Two-fermion states described by the symmetry of the orbital and spin part of their wavefunctions. Arrows show spin projections (up or down), while radii of the spheres indicate the extent of orbitals. For the S state, the radii of the orbitals corresponding to spin-up/-down are the same. For PS, the spin-down orbital is larger, [Eq. (3)], leading to finite spin density and a magnetically-active state.

“non-magnetic” H_f , spin-independent and invariant under the $\mathbf{r}_1 \leftrightarrow \mathbf{r}_2$ interchange. Thus, its eigenstates are also eigenstates of the total carrier spin, and $\varphi_{\sigma\sigma'}(\mathbf{r}_1, \mathbf{r}_2)$ are either symmetric or antisymmetric. The GS of any system of two identical spin-1/2 fermions, described by a spin-independent Hamiltonian, is a singlet with $\sigma + \sigma' = 0$ and $\varphi_{\uparrow\downarrow}(\mathbf{r}_1, \mathbf{r}_2) = \varphi_{\downarrow\uparrow}(\mathbf{r}_2, \mathbf{r}_1)$

[9, 14]. Excited states are either singlets, or triplets with $\varphi_{\sigma\sigma'}(\mathbf{r}_1, \mathbf{r}_2) = -\varphi_{\sigma\sigma'}(\mathbf{r}_2, \mathbf{r}_1)$. Symmetry of the singlet (ground-state) and triplet states is illustrated in Fig. 1.

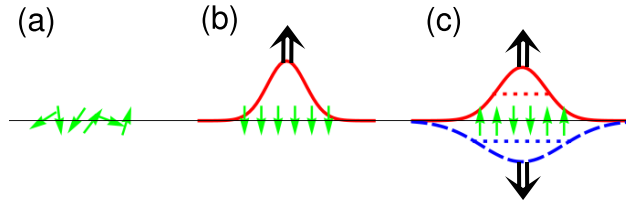


FIG. 2. (color online) Emergence of magnetic bipolarons in QDs. (a) Without carriers, Mn spins (light arrows) are randomly oriented. Double arrows in (b, c) show carrier’s spin projection associated with the orbitals (solid and dashed lines). (b) With 1 carrier, a magnetic polaron forms, lowering the total energy of the system, due to the coupling of the carrier’s spin with the induced Mn magnetization. Mn spins align in one direction. (c) Two carriers assemble in a PS state, forming what we term a magnetic bipolaron. The sign of the Mn-spin projection depends on the sign of the carrier-spin density (difference between dashed and solid curves). The extent of the orbitals (length of dotted lines) is different.

The above classification does not fully apply when H_{ex} is included. We first consider a two-hole system, assuming the Ising exchange, which allows to express any eigenfunction of H as $\psi = \Phi(\{\mathbf{r}_i, s_i\}; \{S_{jz}\}) \prod_j \chi^J(S_{jz})$, where s_i are the spin variables, S_{jz} is the spin projection of j -th impurity, and $\chi^J(S_{jz})$ is an eigenfunction of \hat{S}_{jz} : $\hat{S}_{jz}\chi^J(S_{jz}) = S_{jz}\chi^J(S_{jz})$, where $S_{jz} = -J, \dots, J$ with $J = 5/2$. This separation of ψ (or “classical approximation” for Heisenberg spins) is correct to order $N_{\text{Mn}}^{-1/2}$, where N_{Mn} is the number of Mn spins [15]. It has been widely used in the literature [15, 16]. The separation is exact in the Ising case, so that approximations, such as the variational method used below, are needed only for the carrier subspace. The two-hole Φ depends on $\{S_{jz}\}$ *parametrically*, and it is this coupling that leads to formation of magnetically ordered states. The z -projection of the total carrier spin, Σ , is a good quantum number, so that the Hilbert space splits into three orthogonal subspaces with values $\Sigma = \sigma + \sigma' = 0, 1$ and -1 [17]. We show that the GS is never a singlet, i.e., $\varphi_{\sigma\sigma'}(\mathbf{r}_1, \mathbf{r}_2) \neq \varphi_{\sigma\sigma'}(\mathbf{r}_2, \mathbf{r}_1)$. Instead, it is either a triplet (T) with $|\Sigma| = 1$, or what we term a pseudo-singlet (PS), with $\Sigma = 0$, which reflects its closed-shell character. Unlike the typical singlet, PS leads to ordering of the magnetic moments of the open-shell d -orbitals of Mn, due to breaking of time-reversal symmetry.

Magnetic polarons form by aligning a “cloud” of Mn-spins by a single carrier localized in, e.g., a QD or in an impurity potential [15, 18]. The consequences of presence of two carriers in a magnetic QD are shown in Fig. 2. We predict that, even when the PS is the GS, a magnetic bipolaron is formed, despite vanishing Σ . The finite exchange interaction is

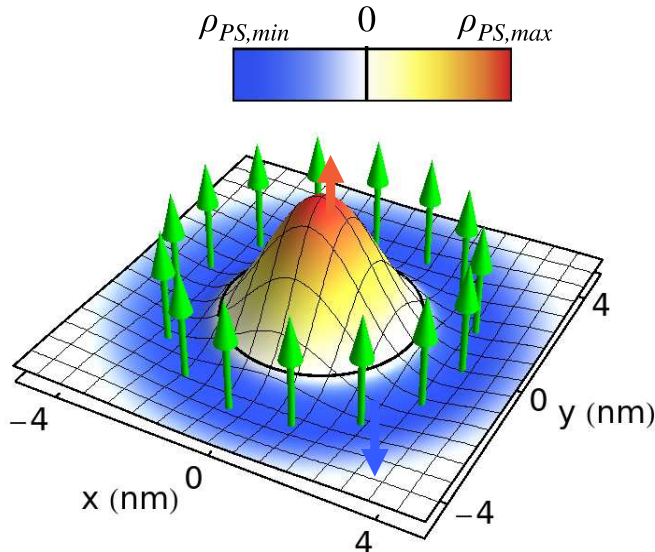


FIG. 3. Spin corral. Colored surface: the hole-spin density ρ_{PS} (arb. units) of PS. Black circle indicates $\rho_{PS}(r = R_0) = 0$. Green arrows: Mn spins, placed at a radius R_C , which maximizes the stability of the ferromagnetic alignment. Red and blue arrows: the more probable hole-spin projections at two positions. The parameters: $\hbar\omega_0 = \Delta_0 = 30$ meV, $Ry^* = \hbar\omega_0/10$, $m^* = 0.5m_0$, $w = 1$ nm [19].

possible due to different Bohr radii of the “up” and “down” orbitals of PS, see the lowest row of Figs. 1 and 2(c). The non-zero exchange and symmetry breaking is particularly obvious for Mn spins arranged in a ring (“spin corral”), Fig. 3. These spins are “ferromagnetically” ordered, their common direction marks one of the two possible states (Mn spins pointing either up or down, perpendicular to the QD plane), corresponding to two stable magnetic-bipolaron solutions separated by an anisotropy barrier. The latter is defined by the strongly anisotropic hole g -tensor.

To analyze magnetic-bipolaron states and the symmetry breaking induced by H_{ex} , we approximate the GS of two interacting holes using two alternative trial wavefunctions. The

first one is the PS ($\Sigma = 0$)

$$\Phi_{\text{PS}} = \frac{1}{\sqrt{2}} [u(\mathbf{r}_1) d(\mathbf{r}_2) \chi_{\uparrow}(1) \otimes \chi_{\downarrow}(2) - u(\mathbf{r}_2) d(\mathbf{r}_1) \chi_{\uparrow}(2) \otimes \chi_{\downarrow}(1)], \quad (3)$$

where $u, d = \sqrt{2/\pi} L_{u,d}^{-1} \exp(-r^2/L_{u,d}^2)$ are single-carrier orbitals corresponding spin “up” and “down” respectively, and $L_{u,d}$ are the variational parameters. Comparing this with Eq. (2), we find $\varphi_{\uparrow\downarrow}(\mathbf{r}_1, \mathbf{r}_2) = 2^{-1/2} u(\mathbf{r}_1) d(\mathbf{r}_2)$ [20]. The second is a $\Sigma = 1$ triplet

$$\Phi_{\text{T}} = \varphi_{\uparrow\uparrow}(\mathbf{r}_1, \mathbf{r}_2) \chi_{\uparrow}(1) \otimes \chi_{\uparrow}(2), \quad (4)$$

where $\varphi_{\uparrow\uparrow}(\mathbf{r}_1, \mathbf{r}_2) = -\varphi_{\uparrow\uparrow}(\mathbf{r}_2, \mathbf{r}_1) = 2/(\pi L_T^3) \times [r_1 e^{i\phi_1} - r_2 e^{i\phi_2}] e^{-(r_1^2 + r_2^2)/L_T^2}$ is the orbital part, in coordinates r, ϕ , and one variational parameter L_T .

The exact treatment of the isotropic g -tensor (for two-electron QDs) requires a large dimension of the Hilbert space. The problem can be circumvented by replacing the Mn-spin operators with classical spin vectors [15]. Then, the two PS and two T solutions (Mn spins pointing up or down, see above), found for holes, form continua (one for PS and one for T), corresponding to Mn spins aligned along arbitrary directions. Any particular solution preserves the form given by Eq. (2) [with z -axis parallel to spontaneous magnetization], and it corresponds to formation of the magnetic bipolaron. The distinct feature of the isotropic case is lack of an anisotropy barrier between different solutions belonging to the same continuum.

Owing to the disk-like shape of typical self-assembled and vertical QDs, the z -dependent Schrödinger equation is factorized out, while the height, h , (along z) of such QDs is usually small. This allows to assume that only the lowest level of this equation is relevant [21]. Thus, for the PS state [recall Eq. (3)], the matrix element of H_{ex} is $E_{ex} = -J_{ex}/(hN_0) \sum_j \rho_{\text{PS}}(\mathbf{R}_j) S_{jz}$, where $\rho_{\text{PS}}(\mathbf{R}_j) = [|u(\mathbf{R}_j)|^2 - |d(\mathbf{R}_j)|^2]/2$. If $L_u \neq L_d$, then $E_{ex} \neq 0$ in a magnetic QD.

In general: For $H_{ex} = 0$ (non-magnetic QDs), PS reduces to a singlet for any Ry^* , because the non-magnetic total energy functional E_S reaches a minimum, E_S^0 , for $L_u^0 = L_d^0 \equiv L_S^0$ (0 indicates a variational minimum). In all studied systems with $H_{ex} \neq 0$, however, $u^0 \neq d^0$, i.e., PS does not reduce to a singlet. Due to its larger spin density, T may become the GS, despite its non-magnetic energy being higher than E_S^0 . (T as the magnetic GS was discussed by Govorov [3, 22]). The functionals $E_{\text{PS,T}}$ reach minima, when Mn spins are antiparallel to hole-spin density.

Due to the exchange coupling, Eq. (1), the total energy functional contains a term linear in the carrier spin density $s(\mathbf{r})$. This term leads to instability of the closed-shell singlet with $s(\mathbf{r}) = 0$. PS, on the other hand, must satisfy a weaker, integral constraint $\int s(\mathbf{r})d\mathbf{r} = 0$. Thus, any small variation of the wavefunction Φ that promotes a non-zero $s(\mathbf{r}) \propto \rho_{\text{PS}}$, while preserving the integral constraint, leads to the instability of the singlet state, because the variations of the kinetic and the Coulomb energies contain only second or higher powers of $s(\mathbf{r})$.

We now describe our results for two particular distributions of Mn spins, starting with homogeneous Mn content x . Figure 4(a) shows the phase diagram of PS and T. The former remains the GS for moderate values of Ry^* and of the saturated Zeeman splitting $\Delta_0 = Jx|J_{ex}|$ [23]. We analyze the GS by considering small variations, δ , of the characteristic lengths from their non-magnetic values L_S^0 and $L_{\text{T,mm}}^0$. We write $L_{u,d} = L_S^0(1 \pm \delta)$ for PS, $L_{\text{T}} = L_{\text{T,mm}}^0(1 + \delta)$ for T, and treat δ as a variational parameter, see Figs. 4(b), (c), and (d). The quantity $\Delta E_{\text{PS}}(\delta) \equiv E_{\text{PS}}(\delta) - E_S^0$, plotted in Fig. 4(b), has two minima corresponding to the two opposite Mn-magnetization profiles mentioned above. The $E_{\text{PS}}^0 - E_S^0$ gap can be an order of magnitude larger for colloidal QDs with a few nm diameter [24], suggesting stability of PS at liquid nitrogen temperatures. Figure 4(c) shows that $\Delta E_{\text{T}}(\delta) \equiv E_{\text{T}}(\delta) - E_{\text{T}}^0$ has δ^2 dependence with a single minimum. Unlike PS, the T wavefunction at the variational minimum is the same as for $H_{ex} = 0$ (i.e., $\delta^0 = 0$), while its energy is lowered by Δ_0 . Hole spin densities and Mn-spin profiles corresponding to PS and T are shown in Figs. 4(d) and (e). The small variation of Φ discussed above is $\propto \delta$. The singlet-PS instability manifests itself as the cusp in the solid line in Fig. 4(b).

Results of a full variational calculation [19], [e.g. Fig. 4(a)], confirm the validity of the δ approximation. By studying the radius at which M_z changes sign, we deduce the magnetization profile for an inhomogeneous x distribution, such that $x(r < R_0) = 0$. Independently of other details of the inhomogeneous distribution, ρ_{PS} has the same sign at all Mn sites, leading to a "ferromagnetic" alignment in a large class of QDs. The same alignment arises when T is the GS. CdSe/(Zn,Mn)Se epitaxial QDs with Mn only at the periphery were created by intentionally introducing Mn in the material surrounding the dot [2, 25]. The placing of individual Mn-ions with a scanning tunnelling microscope [26], is a promising path to realize the "spin-corral". Additionally, $x(r < R_0) = 0$ could be realized in colloidal QDs, where radial segregation of impurities occurs during growth [24]. Such systems show strong

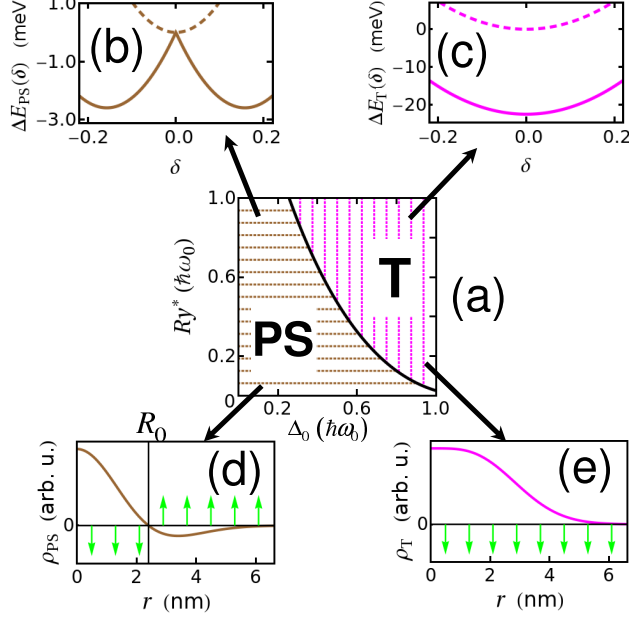


FIG. 4. (color online) (a) Phase diagram of two-hole ground states for homogeneous distribution of Mn. Horizontally (vertically) hatched area indicates the ranges of Ry^* and Δ_0 , for which the ground state is PS (T). PS reduces to singlet only for $\Delta_0 = 0$. (b) for PS, and (c) for T show the non-magnetic (dashed) and total (solid) energies as a function of δ . (d) and (e) show the hole-spin densities (at the corresponding variational minima), along any direction in the $x - y$ plane, with arrows indicating the Mn-spin profiles. The parameters for (b)-(e) are $\hbar\omega_0 = 30$ meV, $\Delta_0 = \frac{3}{4}\hbar\omega_0$, $Ry^* = \hbar\omega_0/10$, $m^* = 0.5m_0$. Vertical line in (d): $R_0 = L_S^0/\sqrt{2}$.

exchange coupling [5], and can be controllably charged [6], thus avoiding fast Auger decay in type-I QDs with two electron-hole pairs. This decay can also be suppressed using core-shell colloidal nanocrystals, equivalent to type-II epitaxial QDs, due to electrons-holes separation [7, 27]. We estimate that for colloidal QDs with ~ 5 nm diameter [24], the singlet-triplet splitting can be ~ 100 meV, resulting in a PS ground state for a wide range of parameters.

PS existence can be also experimentally verified for homogeneous- x QDs, e.g., as a blue shift of interband photoluminescence with magnetic field, B , applied along the z -axis [11]. With increasing B , all the Mn spins will tend to align antiparallel to it, destroying the PS magnetization profile, Fig. 4(d). Thus, PS should increase its energy, while evolving towards the ordinary singlet. This effect could be observed in type-II QDs, where the electrons (unlike the holes) reside in the barrier and do not modify the physical picture. Strong exchange coupling in these QDs is seen as magnetic-polaron formation [7].

Our results can be generalized to closed-shell QDs with more carriers, and to systems, not described by Hamiltonian H_f , typically used for self-assembled [28], vertical [29], or lateral [13] QDs. Shells also form for other confinements [1], e.g., colloidal QDs can be approximately described by spherical or ellipsoidal potential [30]. Closed-shell ($\Sigma = 0$) states appear even for asymmetrical QDs with many carriers [31].

This work was supported by DOE-BES, US ONR, AFOSR-DCT, NSF-ECCS, and CA-REER.

-
- [1] R. Hanson *et al.*, Rev. Mod. Phys. **79**, 1217 (2007); S. M. Reimann and M. Manninen, *ibid.* **74**, 1283 (2002); S. Tarucha *et al.*, *Concepts in Spin Electronics*, ed. S. Maekawa (Oxford Univ. Press, 2006) p. 93.
 - [2] J. Seufert *et al.*, Phys. Rev. Lett. **88**, 027402 (2002).
 - [3] A. O. Govorov, Phys. Rev. B **72**, 075359 (2005).
 - [4] L. Besombes *et al.*, Phys. Rev. Lett. **93**, 207403 (2004); J. Fernández-Rossier and L. Brey, *ibid.* **93**, 117201 (2004); R. M. Abolfath *et al.*, *ibid.* **98**, 207203 (2007); **101**, 207202 (2008).
 - [5] R. Beaulac *et al.*, Science **325**, 973 (2009).
 - [6] S. T. Ochsenbein *et al.*, Nature Nanotech. **4**, 681 (2009).
 - [7] I. R. Sellers *et al.*, Phys. Rev. B **82**, 195320 (2010).
 - [8] We focus on ground states with zero angular momentum.
 - [9] E. Lieb and D. Mattis, Phys. Rev. **125**, 164 (1962).
 - [10] W. Zhang *et al.*, Phys. Rev. B **76**, 075319 (2007).
 - [11] I. Žutić *et al.*, Rev. Mod. Phys. **76**, 323 (2004).
 - [12] P. S. Dorozhkin *et al.*, Phys. Rev. B **68**, 195313 (2003).
 - [13] J. Kyriakidis *et al.*, Phys. Rev. B **66**, 035320 (2002).
 - [14] D. C. Mattis, *The Theory of Magnetism* (Harper & Row, 1965).
 - [15] T. Dietl and J. Spałek, Phys. Rev. B **28**, 1548 (1983); P. A. Wolff, “Diluted Magnetic Semiconductors,” (Academic Press, 1988) p. 413.
 - [16] The separation is similar to that of the Born-Oppenheimer approximation, M. P. Marder, *Condensed Matter Physics* (Wiley, New York, 2000).
 - [17] Similar considerations apply to 2-electron nanostructures placed in magnetic field, see e.g.

- L. Wendler and V. M. Fomin, Phys. Rev. B **51**, 17814 (1995). In those cases the breaking of time-reversal symmetry is not spontaneous.
- [18] I. Terry *et al.*, Phys. Rev. Lett. **69**, 1800 (1992).
- [19] Attached Auxiliary Material to be provided via EPAPS.
- [20] This form of $\varphi_{\uparrow\downarrow}$ and $\rho(\mathbf{R}_j)$ correspond to the unrestricted Hartree-Fock approximation, see L. Piela, *Ideas of Quantum Chemistry* (Elsevier, Amsterdam, 2007).
- [21] We take the corresponding wavefunction to be $1/\sqrt{\hbar}$.
- [22] A. O. Govorov, C. R. Physique **9**, 857 (2008).
- [23] Figure 4(a) also allows to determine which of PS, T is the GS, when the confinement strength, $\hbar\omega_0$, (or the related in-plane size of the QD) changes, while keeping constant Δ_0 and Ry^* . For this, one needs to scale the ratios $\Delta_0/\hbar\omega_0$ and $Ry^*/\hbar\omega_0$. A confinement-driven singlet-triplet transition was noted in [22].
- [24] N. S. Norberg *et al.*, J. Am. Chem. Soc. **128**, 13195 (2006).
- [25] S. Lee *et al.*, J. Cryst. Growth **292**, 311 (2006).
- [26] D. Kitchen *et al.*, Nature **442**, 436 (2006); C. F. Hirjibehedin *et al.*, Science **312**, 1021 (2006).
- [27] V. I. Klimov *et al.*, Nature **447**, 441 (2007).
- [28] G. Kioseoglou *et al.*, Phys. Rev. Lett. **101**, 227203 (2008).
- [29] L. P. Kouwenhoven *et al.*, Rep. Prog. Phys. **64**, 701 (2001).
- [30] G. Cantele *et al.*, Nano Lett. **1**, 121 (2001).
- [31] S. Reimann *et al.*, Eur. Phys. J. D **9**, 105 (1999).